

## Electronic States in $\text{La}_{2-x}\text{Sr}_x\text{CuO}_{4+\delta}$ Probed by Soft-X-Ray Absorption

C. T. Chen,<sup>(1)</sup> F. Sette,<sup>(1)</sup> Y. Ma,<sup>(1)</sup> M. S. Hybertsen,<sup>(1)</sup> E. B. Stechel,<sup>(2)</sup> W. M. C. Foulkes,<sup>(1)</sup> M. Schluter,<sup>(1)</sup> S-W. Cheong,<sup>(1)</sup> A. S. Cooper,<sup>(1)</sup> L. W. Rupp, Jr.,<sup>(1)</sup> B. Batlogg,<sup>(1)</sup> Y. L. Soo,<sup>(3)</sup> Z. H. Ming,<sup>(3)</sup> A. Krol,<sup>(3)</sup> and Y. H. Kao<sup>(3)</sup>

<sup>(1)</sup>*AT&T Bell Laboratories, 600 Mountain Avenue, Murray Hill, New Jersey 07974*

<sup>(2)</sup>*Condensed Matter Theory Division 1151, Sandia National Laboratories, Albuquerque, New Mexico 87185*

<sup>(3)</sup>*Department of Physics, State University of New York, Buffalo, New York 14260*

(Received 14 September 1990)

Oxygen *K*-edge absorption spectra of carefully characterized  $\text{La}_{2-x}\text{Sr}_x\text{CuO}_{4+\delta}$  samples were measured using a bulk-sensitive fluorescence-yield-detection method. They reveal two distinct pre-edge peaks which evolve systematically as a function of Sr concentration. The measured spectra are quantitatively described by calculations based on the Hubbard model, including local Coulomb interactions and core-hole excitonic correlations. The absorption data are consistent with a description of electronic states based on a doped charge-transfer insulator.

PACS numbers: 78.70.Dm, 71.30.+h, 74.70.Vy, 75.30.Et

The nature of carriers in the cuprates which exhibit high- $T_c$  superconductivity remains an open and controversial problem. Spectroscopic probes with chemical specificity, e.g., resonant photoemission, x-ray absorption, and electron-energy-loss spectroscopy (EELS), have led to important insight into the character of the carriers responsible for conduction. For example, the role of strong local electronic correlations has been highlighted<sup>1</sup> and the predominantly O *2p* character of carriers in the hole-doped materials has been established.<sup>2,3</sup> However, a detailed experimental picture of the evolution of the electronic states as a function of excess hole concentration (e.g., Sr concentration in  $\text{La}_{2-x}\text{Sr}_x\text{CuO}_4$ ) is still lacking. Furthermore, models for the electronic structure of these materials must confront such experimental data. In particular, it has been controversial as to whether models based on a doped insulator or a bandlike metal best fit the available data.

In this paper we describe soft-x-ray absorption measurements at the O *K* edge in carefully characterized samples of  $\text{La}_{2-x}\text{Sr}_x\text{CuO}_{4+\delta}$  using a bulk-sensitive fluorescence-yield-detection method. As a function of Sr concentration, two "prepeaks" are observed: The lower peak, absent for  $x=0$ , grows in intensity with the Sr concentration, while the upper peak loses intensity. The total intensity in the prepeak region increases with  $x$ . The energy separation between the two peaks is comparable to the optical gap in the insulating phase and monotonically increases with  $x$ . These trends are quantitatively explained starting from an extended three-band Hubbard model<sup>4</sup> whose parameters have been derived from quantum-chemical calculations.<sup>5</sup> The local core-hole potential is included which introduces excitonic correlations. The upper peak is identified with transitions into the upper Hubbard band (largely Cu *d* character), while the lower peak emerges with the introduction of carriers into the charge-transfer band (mostly O *p*

character). This study demonstrates that the soft-x-ray absorption data are consistent with a picture of low-energy electronic states derived from a doped charge-transfer insulator over the entire range of carrier concentration from the very dilute, insulating regime well into the metallic, superconducting regime.

High-density ceramic  $\text{La}_{2-x}\text{Sr}_x\text{CuO}_4$  samples with  $x=0.00, 0.02, 0.04, 0.07, 0.10,$  and  $0.15$  as well as an oxygen-enriched  $\text{La}_2\text{CuO}_{4+\delta}$  sample were prepared as described previously.<sup>6</sup> The amount of extra oxygen,  $\delta$ , was uncertain; however, estimates from the Hall effect and measurements of  $T_N$  suggest  $\delta \sim 0.005$ .<sup>6</sup> The superconducting properties were characterized by magnetic-susceptibility measurements and did not change as a result of the soft-x-ray absorption measurements. The samples with  $x=0.00, 0.02,$  and  $0.04$  are insulators. Those with  $x=0.07, 0.10,$  and  $0.15$  are superconductors with  $T_c$  (Meissner fraction,  $H=10$  Oe) of 16 K (20%), 31 K (39%), and 38 K (55%), respectively. Scanning electron microscopy and transmission electron microscopy showed that all samples exhibited extremely good crystallinity and homogeneity, almost as good as high-quality single crystals.

The oxygen *K*-edge photoabsorption measurements were performed using the AT&T Bell Laboratories Dragon high-resolution soft-x-ray beam line at the National Synchrotron Light Source at Brookhaven National Laboratory.<sup>7</sup> For these measurements, the monochromator resolution was set at 0.25 eV. Both the oxygen *K $\alpha$*  fluorescence yield (FY) and *KLL* Auger total electron yield (TEY) were monitored simultaneously using a low-pressure parallel-plate avalanche chamber<sup>8</sup> and a channel electron multiplier, respectively. The probing depth for FY is  $\sim 2500$  Å around the O *K* edge and that for TEY is a few hundred angstroms. By comparing the FY and TEY data, the surface quality of the sample can be characterized.<sup>9</sup> Three different treatments of the

sample surfaces (freshly grown, polished in air, the scraped *in vacuo*) have been compared. Whereas polishing with alumina powder suspended in methanol always recovered the *bulk-sensitive* FY spectra observed for freshly grown samples, we found that scraping *in vacuo* can seriously damage the surface. To obtain high accuracy, the spectra were taken one scan at a time for every sample and repeated at least thirty times. The total number of counts in the prepeak area is of the order of  $3 \times 10^5$ , and the relative peak positions are precise to within  $\pm 40$  meV.

Figure 1(a) shows the oxygen *K*-edge FY spectra of  $\text{La}_{2-x}\text{Sr}_x\text{CuO}_4$  for  $x$  between 0 and 0.15, and for one oxygen-enriched sample,  $\text{La}_2\text{CuO}_{4.005}$ . The spectra are normalized to have the same area in the energy range between 534 and 560 eV (not fully shown in the figure). Two distinct peaks (labeled *A* and *B*) are observed at photon energies around 528.8 and 530.3 eV showing a separation comparable to the optical gap (1.8 eV).<sup>10</sup> Interestingly, the oxygen-enriched sample exhibits the same two-peak structure. To determine the spectroscop-

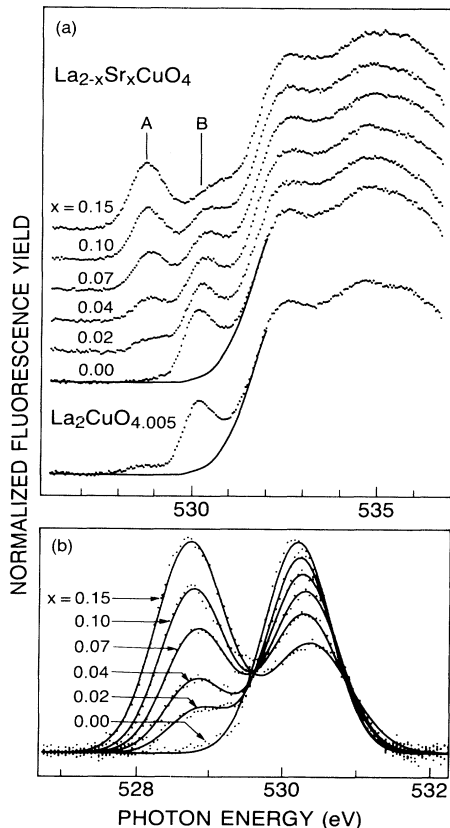


FIG. 1. (a) Normalized fluorescence yield at the O *K* edge of  $\text{La}_{2-x}\text{Sr}_x\text{CuO}_{4+\delta}$ . The solid curves are the common background described in the text. (b) The difference between the data of  $\text{La}_{2-x}\text{Sr}_x\text{CuO}_4$  and the common background. The solid lines are the fitted curves using two Gaussian line shapes.

ic parameters (peak position, width, and area), the increasing background between 530 and 532 eV has been represented by an analytic function shown as the solid curves (a combination of Gaussian and linear backgrounds) which is the *same* in all cases. Figure 1(b) shows the data in the pre-edge region after subtraction of the background. The data in Fig. 1(b) are best fitted by two Gaussian line shapes as shown by the solid curves.

The three-band extended Hubbard model<sup>4</sup> focuses on the Cu  $3d(x^2-y^2)$  and the O  $2p\sigma(x,y)$  orbitals as describing both the local spins responsible for antiferromagnetism as well as the carriers. Parameters for this model have been calculated which well represent the specific properties of the cuprates.<sup>5</sup> The x-ray absorption process is described by a transition operator which creates an O  $1s$  core hole and annihilates an O  $2p$  hole *on the same site*. In the final states, the core hole interacts with valence holes (the  $p$  orbital on the O site of the core hole and the  $d$  orbital on the neighboring Cu sites) via the Coulomb interaction which we represent by an on-site  $U_{cp} = 6$  eV and a nearest-neighbor  $U_{cd} = 1.2$  eV.<sup>11</sup> The  $U_{cd}$  leads to excitonic renormalization of the gap between the peaks. The x-ray absorption cross section is calculated for finite clusters using Lanczos (exact diagonalization) methods. For the full three-band Hubbard model, cluster size is severely restricted. To consider larger clusters, we take advantage of the previously demonstrated result that the low-energy electronic states of the cuprates can be well represented by an effective one-band Hubbard model.<sup>12,13</sup> The predominantly Cu  $d$ -like holes are represented by singly occupied sites while the extra O  $p$ -like holes introduced by doping are the doubly occupied sites. The Hubbard  $U$  reflects the charge-transfer gap. Here we extend this approach by mapping the O *K*-edge absorption process into the same one-band model.<sup>14</sup> This requires representing both the core-hole potential as well as the transition operator in the one-band model. Tests show that the calculated cross section using this one-band model accurately reproduces the results from the full three-band model. Here, a cluster with 10 Cu sites with periodic boundary conditions is used.

The calculated cross section for O *K*-edge absorption is shown in Fig. 2(a) in the region of the prepeaks, where the model applies, for varying numbers of extra holes. The calculated spectra are convoluted with a Gaussian of  $\text{FWHM} = 0.5$  eV to represent instrumental resolution, estimated phonon broadening, and the O  $1s$  lifetime (0.2 eV in the free ion). The peak position is aligned to experiment for  $x = 0$ . With no extra holes, the spectrum shows a dominant peak due to transitions into the upper Hubbard band. Upon introduction of extra holes, a new peak due to transitions into the charge-transfer band appears at lower energies which grows in intensity, shifts to lower energy, and splits. At the same time, the upper peak reduces in intensity and shifts to higher energy.

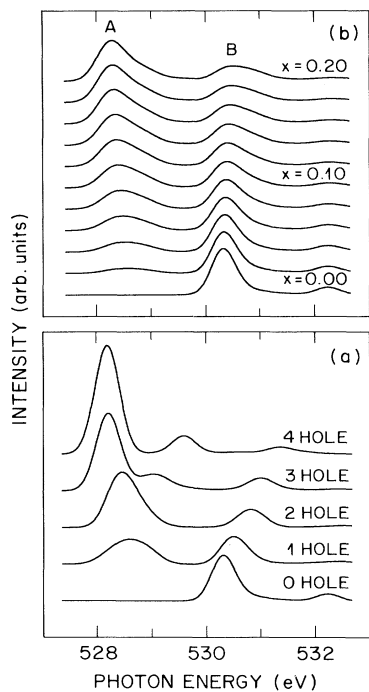


FIG. 2. (a) Calculated O  $K$ -edge absorption cross section for the indicated fixed number of excess holes in a planar unit cell containing 10 Cu sites. (b) Calculated O  $K$ -edge absorption cross section as a function of energy for the indicated range of average excess hole concentrations.

This crossover of intensity has been seen in Li-doped NiO.<sup>15</sup> The qualitative explanation given in Ref. 15 applies here as well. The peak separation for one extra hole is renormalized from the calculated charge-transfer gap by 0.8 eV due to the core-hole excitonic correlations. Further, the core-hole potential leads to a classic two-dimensional exciton peak derived from the empty Cu  $d$ -like states, the sharp upper peak. The shape of the lower peak, particularly the splitting observed for three and four holes, reflects the underlying density of states for the present 10-site cluster. The core-hole potential transfers strength to the threshold region (low-energy side) exactly as one expects for the core-hole excitonic correlations in a metal.

The calculated spectra in Fig. 2(a) already exhibit qualitatively the features of the measured spectra. A closer comparison requires understanding the role of fluctuations in carrier concentration in the region near the core hole. First, the calculation for one extra hole in the 10-site cell is *not* equivalent to 10% carrier concentration in an extended system. For a 10-site box in a *metallic* system, fluctuations with zero, one, two, etc., extra carriers in the box can be expected. An approximate solution to this technical problem is to do a suitable average of the spectra calculated in the small cell with various numbers of excess holes. Second, the impurity po-

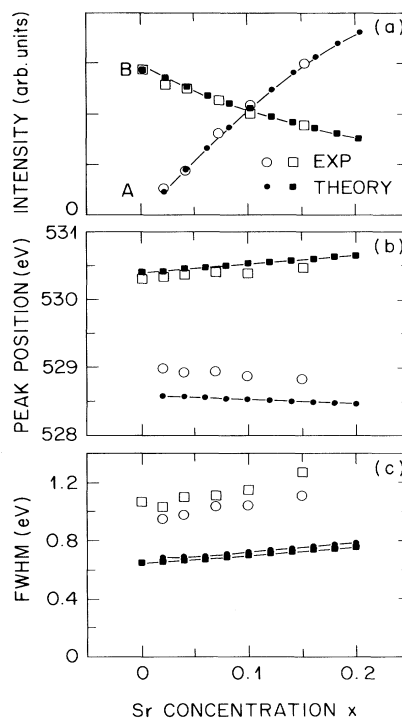


FIG. 3. Comparison of experiment and theory for (a) peak intensity, (b) peak position, and (c) peak width as a function of Sr concentration.

tential is a source of fluctuations. In the dilute (insulating) limit, the impurity (Sr) potential binds the extra hole with a radius of about 6 Å and an estimated binding energy of 0.5–0.7 eV.<sup>16</sup> The absorption spectrum for a given O atom, being sensitive to local carrier density, depends on the positions of the nearby Sr impurities. The total spectrum is then obtained by taking an average over possible local Sr configurations. Calculations with model impurity potentials show that the absorption spectra depend weakly on the impurity potential. This follows from the impurity-derived chemical shifts of the core level, the local nature of the probe, and the average over impurity configurations. Peak positions and intensities are largely unaffected, while the width is increased. Therefore, the impurity potential can be approximately neglected. However, the *distribution* of impurities leads to fluctuations in the number of carriers in the cell. Thus, the spectrum for given  $x$  is a weighted average of the individual spectra in Fig. 2(a). The weights are derived from the statistical occurrence of Sr atoms in the 10-site cell for each  $x$ . Even in the metallic regime, results are close to those found using weights derived from a model for metallic fluctuations. This model does not describe the region near the metal-insulator transition *per se*, but provides a smooth interpolation.

Spectra calculated for a sequence of carrier concentra-

tions are shown in Fig. 2(b) for  $x$  in the range 0.00–0.20. The theoretical results exhibit noticeably asymmetric peaks but otherwise strongly resemble the measured spectra. A direct comparison is shown in Fig. 3. For the integrated peak intensity [Fig. 3(a)], the theory is scaled to experiment for the single peak in the spectrum for  $x=0$ . All other relative peak intensities are fixed by the calculated transition matrix elements. The theory accurately reproduces the changes in intensity as a function of dopant concentration.<sup>17</sup> The calculated first moment is compared with the measured peak position in Fig. 3(b). The systematic dispersion of the peaks is also well reproduced. The peak positions shift as carrier density increases due to the increasing weight of multiple hole-derived spectra in Fig. 2(a). Physically, the lower peak shifts as more empty states are available with increased doping, while the upper peak shifts due to the interference effects discussed in Ref. 15. The 0.4-eV discrepancy between the calculated and measured peak separation may result from several sources, including uncertainties in theoretical values for the local  $p$ - $d$  energy separation and core-hole interaction energies or finite-size effects. Finally, the measured FWHM is compared to the calculation (broadened) in Fig. 3(c). The theoretical linewidth is smaller than the measured one. Inclusion of the impurity potential would broaden the lower peak. The O  $1s$  lifetime in the solid may be significantly shorter than in the free atom due to the increased number of local O  $2p$  electrons as well as possible intersite Auger processes. This may account for much of the overall discrepancy.

The present experimental and theoretical results offer strong evidence that the picture of electronic states derived from a doped charge-transfer insulator is well supported by x-ray absorption measurements for carrier concentrations extending into the metallic (superconducting) range. The energy separation of the two pre-edge peaks observed in the spectra for doped materials is the charge-transfer gap, renormalized by core-hole excitonic correlations. The spectra evolve smoothly with hole concentration and no break is observed near the resistively measured onset of metallic behaviors (near  $x=0.06$ ). This is in agreement with earlier EELS measurements,<sup>18</sup> which also showed a smooth crossover near the metal-insulator transition.

It is a pleasure to acknowledge useful discussions with Professor G. A. Sawatzky and Dr. D. R. Jennison and the technical assistance of E. E. Chaban, Dr. G. C. Smith, and Dr. C. Alstadi. Work done at the National

Synchrotron Light Source was supported by the U.S. DOE under Contract No. DE-AC02-76CH00016, at Sandia National Laboratories by the U.S. DOE under Contract No. DE-AC04-76DP00789, and at State University of New York at Buffalo by AFOSR Grant No. AFOSR-88-0095 and by the U.S. DOE under contract No. DE-FG02-87ER45283.

<sup>1</sup>A. Fujimori, E. Takayama-Muromachi, Y. Uchida, and B. Okai, *Phys. Rev. B* **35**, 8814 (1987); Z.-X. Shen *et al.*, *Phys. Rev. B* **36**, 8414 (1987); D. van der Marel, J. van Elp, G. A. Sawatzky, and D. Heitmann, *Phys. Rev. B* **37**, 5136 (1988).

<sup>2</sup>J. A. Yarmoff *et al.*, *Phys. Rev. B* **36**, 3967 (1987); N. Nucker *et al.*, *Phys. Rev. B* **37**, 5158 (1988).

<sup>3</sup>A. J. Arko *et al.*, *Phys. Rev. B* **40**, 2268 (1989); J. W. Allen *et al.*, *Phys. Rev. Lett.* **64**, 595 (1990).

<sup>4</sup>V. J. Emery, *Phys. Rev. Lett.* **58**, 3759 (1987); C. M. Varma, S. Schmitt-Rink, and E. Abrahams, *Solid State Commun.* **62**, 681 (1987).

<sup>5</sup>A. K. McMahan, R. M. Martin, and S. Satpathy, *Phys. Rev. B* **38**, 6650 (1989); M. S. Hybertsen, M. Schluter, and N. E. Christensen, *Phys. Rev. B* **39**, 9028 (1989).

<sup>6</sup>S.-W. Cheong, M. F. Mundle, J. D. Thompson, and Z. Fisk, *Phys. Rev. B* **39**, 6567 (1989); M. C. Aronson *et al.*, *Phys. Rev. B* **39**, 11445 (1989).

<sup>7</sup>C. T. Chen and F. Sette, *Rev. Sci. Instrum.* **60**, 1616 (1989); *Phys. Scr.* **T31**, 119 (1990).

<sup>8</sup>Similar to the design of G. C. Smith, A. Krol, and Y. H. Kao, *Nucl. Instrum. Methods Phys. Res., Sect. A* **291**, 135 (1990).

<sup>9</sup>A. Krol *et al.*, *Phys. Rev. B* **42**, 2635 (1990).

<sup>10</sup>J. Orenstein *et al.*, *Phys. Rev. B* **36**, 8892 (1987); S. Tajima *et al.*, *J. Opt. Soc. Am.* **6**, 475 (1989).

<sup>11</sup>The response to a frozen O  $1s$  core hole was calculated using the local-density functional approach and the Coulomb interaction parameters were extracted. See Ref. 5.

<sup>12</sup>P. W. Anderson, *Science* **235**, 1196 (1987); F. C. Zhang and T. M. Rice, *Phys. Rev. B* **37**, 3759 (1988).

<sup>13</sup>M. S. Hybertsen, E. B. Stechel, M. Schluter, and D. R. Jennison, *Phys. Rev. B* **41**, 11068 (1990), and references therein. Here,  $U=4.1$  eV better represents the charge-transfer gap.

<sup>14</sup>M. S. Hybertsen, E. B. Stechel, W. M. C. Foulkes, and M. Schluter (to be published).

<sup>15</sup>P. Kuiper *et al.*, *Phys. Rev. Lett.* **62**, 221 (1989); H. Eskes and G. A. Sawatzky, *Phys. Rev. B* (to be published).

<sup>16</sup>K. Rabe and R. Bhatt (unpublished).

<sup>17</sup>For an 8-site cluster, the lower peak intensity is unchanged while the upper peak is reduced by  $\sim 15\%$ .

<sup>18</sup>H. Romberg, M. Alexander, N. Nucker, P. Adelman, and J. Fink, *Phys. Rev. B* **42**, 8768 (1990).